

Measurement of the Muon Magnetic anomaly to 0.20 ppm by the Muon $g - 2$ experiment at Fermilab

L. Cotrozzi^{1,2*} on behalf of the Muon $g - 2$ Collaboration

¹ Department of Physics, University of Liverpool, UK

² INFN, Pisa, Italy

* lcotrozz@hep.ph.liv.ac.uk

July 4, 2024



The 17th International Workshop on Tau Lepton Physics
Louisville, USA, 4-8 December 2023
doi:10.21468/SciPostPhysProc.?

Abstract

The Muon $g - 2$ experiment at Fermilab aims to measure the muon magnetic moment anomaly, $a_\mu = (g - 2)/2$, with a final accuracy of 0.14 parts per million (ppm). The experiment's first result was published in 2021, based on data collected in 2018, and in 2023 a new result was published based on two more years of data taking, 2019 and 2020. The combination of the two results from Fermilab and the previous one from Brookhaven National Laboratory brought the uncertainty on the experimental measurement of a_μ to the unprecedented value of 0.19 ppm. This paper will present details about the improvements of statistical and systematic uncertainties on a_μ since the 2021 result.

1 The magnetic moment of the muon

The gyromagnetic ratio g is a factor of proportionality between the magnetic moment $\vec{\mu}$ of a charged particle and its spin \vec{S} : $\vec{\mu} = g(e/2m)\vec{S}$. From Dirac's equation, muons should have a value of g equal to 2; but in the Standard Model (SM) framework of quantum field theories, g is corrected to a slightly higher value than 2 from QED, weak interactions and QCD. The muon magnetic anomaly is defined as the fractional difference of g_μ from 2: $a_\mu = (g_\mu - 2)/2$. Figure 1 presents the experimental values of a_μ as measured by BNL E821 [1] and FNAL E989 in Run-1 (2021) [2] and Run-2/3 (2023) [3, 4]. The contribution to a_μ from the quantum chromodynamics (QCD) sector amounts to ~ 60 parts per million (ppm) and carries the largest uncertainty. The major contribution comes from hadronic vacuum polarization (HVP), where the energy scale is of the order of the muon mass, well below the region where QCD can be studied perturbatively: a dispersion relation approach can be used to evaluate the contribution, using the experimental hadronic cross section of e^+e^- as an input. Lattice QCD can also be used to determine the HVP contribution to a_μ using an ab-initio calculation. In 2020, the Theory Initiative recommended a value for the theoretical prediction of a_μ in a White Paper [5], based on the dispersive approach. This led to a discrepancy between the experimental value and the SM calculation from the Muon $g - 2$ Theory Initiative: $a_\mu^{exp} - a_\mu^{SM} = (249 \pm 48) \cdot 10^{-11}$, with a significance of 5.1σ . In recent years, puzzles in the theoretical prediction of a_μ have arisen, which prevent a solid comparison with the experimental value. In 2021, the BMW collaboration presented a prediction of a_μ^{HVP} with lattice QCD with an uncertainty of 0.8% [6], which was in tension with the dispersive approach. Other collaborations which use a lattice

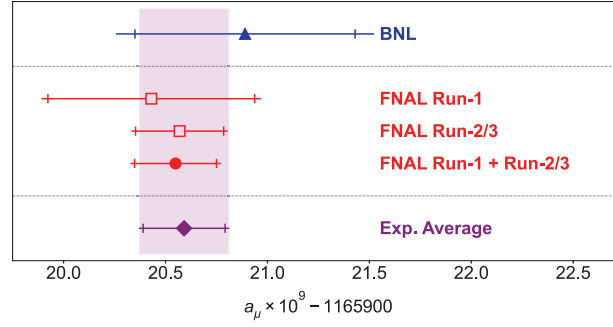


Figure 1: Measured values of a_μ from BNL and FNAL, and new experimental average. The inner tick marks indicate the statistical contribution to the total uncertainties [3].

33 approach are working to reach a similar uncertainty on a_μ^{HVP} as BMW, in order to verify the
 34 current prediction. On top of that, in 2023 the measurement of the $e^+e^- \rightarrow \pi^+\pi^-$ cross section
 35 with the CMD-3 detector [7] resulted in a hadronic contribution to a_μ that was significantly
 36 larger than the value obtained from previous measurements.

37 2 The Muon $g - 2$ (E989) experiment at Fermilab

38 In the Muon $g - 2$ experiment, a spin-polarized beam of 3.1 GeV positively charged muons
 39 is injected into a ~ 7 m radius superconducting storage ring, that produces a vertical and
 40 uniform, at the ppm level, 1.45 T magnetic field. Electrostatic quadrupole (ESQ) plates provide
 41 weak focusing for vertical confinement. In the storage ring, muons precess with cyclotron
 42 frequency ω_C , and their spin also precesses around the direction of the magnetic field, with
 43 frequency ω_S . Given e and m the charge and mass of muons, respectively, the anomalous
 44 precession frequency ω_a is defined as:

$$\vec{\omega}_a \equiv \vec{\omega}_S - \vec{\omega}_C = -\frac{e}{m} \left[a_\mu \vec{B} - a_\mu \left(\frac{\gamma}{\gamma + 1} \right) (\vec{\beta} \cdot \vec{B}) \vec{\beta} - \left(a_\mu - \frac{1}{\gamma^2 - 1} \right) \frac{\vec{\beta} \times \vec{E}}{c} \right]. \quad (1)$$

45 \vec{E} is the electric field from ESQ, \vec{B} the magnetic dipole, $\vec{\beta}$ the muons' speed and γ their Lorentz
 46 factor. In the Muon $g - 2$ experiment, only the first term in square brackets is relevant in the
 47 first approximation, because muons travel perpendicularly to the B-field and $\gamma \approx 29.3$ is such
 48 that the last parenthesis vanishes. When only the first term is considered, the equation for $\vec{\omega}_a$
 49 becomes $\omega_a = a_\mu (e/m) B \simeq 1.43 \text{ rad}/\mu\text{s}$, with a direct proportionality between a_μ and ω_a/B .
 50 Expressing the magnetic field in terms of the Larmor precession frequency of free protons, via
 51 $\hbar\omega_p = 2\mu_p |\vec{B}|$, the formula used for a_μ is in Equation (2):

$$a_\mu = \left[\frac{f_{\text{clock}} \cdot \omega_a (1 + C_e + C_p + C_{pa} + C_{dd} + C_{ml})}{f_{\text{calib}} \cdot \langle \omega'_p(\vec{r}) \times M(\vec{r}) \rangle (1 + B_q + B_k)} \right] \times \frac{\mu_p(T_r)}{\mu_e(H)} \frac{\mu_e(H)}{\mu_e} \frac{m_\mu}{m_e} \frac{g_e}{2} \quad (2)$$

52 Inside the square brackets, at the numerator, ω_a is the anomalous precession frequency, mea-
 53 sured as described in Subsection 2.1; the factor f_{clock} , unknown to the Muon $g-2$ collaboration,
 54 is set to introduce a blinding in the range ± 25 ppm; the measurement of the magnetic field
 55 factor at the denominator $f_{\text{calib}} \cdot \langle \omega'_p(\vec{r}) \times M(\vec{r}) \rangle$ is described in Subsection 2.2, where the
 56 prime symbol ' indicates shielded (not free) protons; the factors C_i and B_i account for beam
 57 dynamics and magnetic transients effects, respectively, and are described in Subsection 2.3.
 58 The external factors are known to 25 parts per billion (ppb) [4], and they are: the shielded

59 proton-to-electron magnetic moment $\mu_p(T_r)/\mu_e(H)$, measured at the reference temperature of
 60 $T_r = 34.7^\circ\text{C}$; the QED factor $\mu_e(H)/\mu_e$, which is the ratio of the magnetic momentum of the
 61 electron in a hydrogen atom to the magnetic momentum of the free electron in vacuum; the
 62 ratio between the muon and electron masses m_μ/m_e , and the electron g-factor g_e .

63 2.1 ω_a measurement

64 24 electromagnetic calorimeters are placed along the inner radius of the Muon $g - 2$ storage
 65 ring, each composed of an array of 6×9 lead-fluoride crystals, that can detect positrons from
 66 μ^+ decays. Positrons generate Cherenkov light in the crystals, which is detected by SiPMs,
 67 converted into a voltage signal and recorded for analysis. From template fits on crystal pulses,
 68 positrons' energies and times of arrival are reconstructed. Since muons decay weakly, there
 69 is a correlation between the positron energy in the center-of-mass frame and the direction of
 70 the muon spin. In the lab frame, the time distribution of positrons above a given threshold is
 71 given by Equation (3):

$$N(t) = N_0 e^{-t/\gamma\tau} [1 + A_0 \cos(\omega_a t + \phi_0)], \quad (3)$$

72 where N_0 is a normalization parameter, A_0 the amplitude of the oscillation, ϕ_0 the initial phase,
 73 and $\gamma\tau$ is the muon lifetime in the lab frame. We choose a threshold of 1.7 GeV that minimizes
 74 the statistical uncertainty on ω_a . In alternative, it is possible to weight the contribution of
 75 each event by the asymmetry A , which depends on the positron energy E , which enable us to
 76 lower the threshold down to 1 GeV thus increasing the statistics and reducing the uncertainty.
 77 The complete ω_a fit function includes terms which account for the muon losses and beam
 78 dynamics frequencies; the number of floating parameters depends on the analysis group, and
 79 is typically between 20 and 30 [4].

80 2.2 Magnetic field measurement

81 During data taking, the proton precession ω'_p is constantly measured by 378 nuclear magnetic
 82 resonance (NMR) fixed probes, placed along the ring above and below the storage volume.
 83 About once every three days, a so-called *trolley run* is performed with no muon beam stored,
 84 where a cylinder equipped with 17 NMR probes is moved on rails inside the vacuum chamber
 85 with the purpose of producing a three dimensional map of the magnetic field that the muons
 86 experience. The fixed probes monitor the field stability between two consecutive trolley runs.
 87 The NMR technique uses a radio frequency (RF) pulse (~ 61 MHz) applied to the proton sam-
 88 ple in petroleum jelly, in order to rotate the proton spin of 90° such that it lies in the plane
 89 perpendicular to the storage ring B-field. When the RF pulse is turned off, the sample polar-
 90 ization starts precessing in the storage ring magnetic field until the net magnetization of the
 91 sample returns to being aligned with the external field. Pickup coils oriented perpendicularly
 92 to the magnetic field are connected to waveform digitizers that save the current induced in
 93 the coils by the precessing protons: this current is the so-called free induction decay signal,
 94 and measuring it over time gives information about the magnetic field. The Larmor precession
 95 frequency is about 61.79 MHz in the $g - 2$ storage ring, and it is mixed down to ~ 50 kHz prior
 96 to digitization. Both the trolley and fixed probes are calibrated with a water-sample probe
 97 , that can be positioned in the same locations as the trolley probes. This step provides the
 98 absolute calibration of the field measurement represented by the term f_{calib} in Equation (2).
 99 The term f_{calib} includes the effects related to the diamagnetic shielding of the petroleum jelly
 100 NMR probes caused by the trolley body and shape. The final value of ω'_p required in Equation
 101 (2) is the average magnetic field $\tilde{\omega}'_p$ experienced by the muons as they precess around the
 102 ring, obtained by weighting the ω'_p map with the muon beam distribution $M(\vec{r}, t)$ measured
 103 by two straw tracker detectors, and by integrating over time and space [4].

104 2.3 Beam dynamics and transient fields corrections

105 The anomalous precession frequency ω_a is extracted from wiggle plot fits. The quantity that
 106 we measure, indicated with ω_a^m in Equation (2), is not truly the precession frequency ω_a due to
 107 beam dynamics effects which modify the simple relation $\omega_a = a_\mu(e/m)B$. The electric field C_e
 108 and pitch C_p corrections make the spin precess slower than in the ideal experiment; the phase
 109 acceptance C_{pa} , differential decay C_{dd} and muon losses C_{ml} corrections affect the average
 110 muon initial phase ϕ of Equation (3) over fill time, thus biasing ω_a . The corrections B_k and
 111 B_q arise because, during muon storage, two time-dependent magnetic fields are induced by
 112 the pulsed magnetic and electric fields from the kicker and quadrupoles that are synchronized
 113 with each muon fill. These transient magnetic fields are not present during the trolley runs;
 114 the fixed probes only measure the field at time intervals of ~ 1 s asynchronously with respect
 115 to muon injection, whereas the fast transients change on the μ s timescales, so they must be
 116 included as corrections to ω_p at the denominator of Equation (2). In paragraphs V and VI.G
 117 of the PRD article [4], these corrections are described in detail: their overall contribution is
 118 0.6 ppm, which is ~ 5 times larger than the uncertainty we plan to quote with the full statistics.

119 3 Improvements from Run-1 to Run-2/3 results

120 There were several improvements after the Run-1 (2021) result, in terms of running condi-
 121 tions, analysis techniques and systematic studies. First of all, in Run-2/3 we collected 4.7 times
 122 the number of Run-1 decay positrons, which reduced the statistical uncertainty on ω_a by a fac-
 123 tor ~ 2.2 , and allowed to perform more detailed studies on one of the systematic effects that
 124 dominated the Run-1 results, namely the aliased Coherent Betatron Oscillation of the muon
 125 beam. During Run-1 there were two damaged resistors in the ESQ plates, fixed before Run-2,
 126 which strongly affected the stability of beam oscillations and enhanced the phase acceptance
 127 correction C_{pa} and its uncertainty. Towards the end of Run-3, the non-ferric fast kicker mag-
 128 net, which is necessary to store the muon beam at the time of injection, was upgraded in order
 129 to achieve the optimal kick, consequently lowering the electric field correction C_e . On the ω_a
 130 side, new reconstruction algorithms were employed to reduce the pileup systematic uncer-
 131 tainty, which dominated in Run-1. In addition, a new Asymmetry-weighted ratio method was
 132 developed, which consisted in subdividing data into two wiggle plots, weighting the positron
 133 events and shifting them in time appropriately such that the ratio between their difference and
 134 their sum cancelled the muon exponential decay. This method preserved statistical power in
 135 the ω_a fit, whilst reducing sensitivity to many systematics. On the field side, more measure-
 136 ments of the quadrupole transients and improvements in the magnetometer that measured the
 137 kicker transients resulted in smaller systematic uncertainties for the respective terms B_q and
 138 B_k . With all these improvements, in Run-2 and Run-3 the statistical and systematic uncertain-
 139 ties on a_μ were reduced with respect to Run-1, from 434 ppb to 201 ppb and from 157 ppb to
 140 70 ppb, respectively. Figure 2 shows the improvements in individual terms of Equation (2).

141 4 Conclusion

142 The goal of the Muon $g-2$ experiment at Fermilab is to measure the muon magnetic anomaly
 143 a_μ at the 0.14 ppm level of precision, a fourfold improvement with respect to the previous
 144 experiment at BNL. Combining the experiment's results of 2021 and 2023 and the previous
 145 BNL result, the new experimental measurement of a_μ has reached the unprecedented precision
 146 of 0.19 ppm; in the 2023 result, the systematic uncertainty reached 70 ppb, surpassing the goal

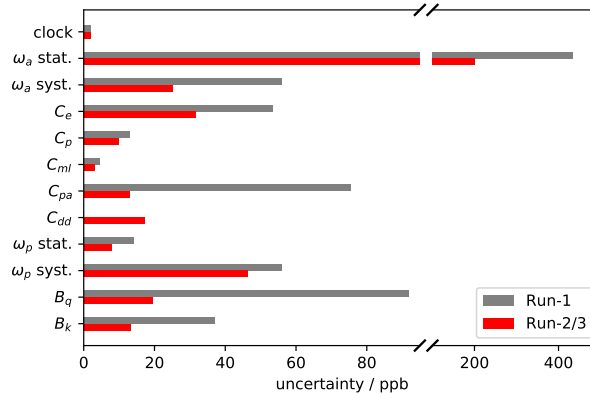


Figure 2: Comparison of statistical and systematic uncertainties between the Run-1 [2] and the Run-2/3 [3, 4] results.

147 of 100 ppb [8], and with the ongoing analysis of the last three datasets, Run-4/5/6, we expect
 148 to reach the goal of 100 ppb in statistical uncertainty.

149 Acknowledgements

150 This work was supported in part by the US DOE, Fermilab, the Istituto Nazionale di Fisica
 151 Nucleare and the European Union Horizon 2020 research and innovation programme under
 152 the Marie Skłodowska-Curie grant agreements No. 101006726, No. 734303.

153 References

- 154 [1] G. W. Bennett *et al.* (Muon $g - 2$ collaboration), *Final report of the E821 muon*
 155 *anomalous magnetic moment measurement at BNL*, Phys. Rev. D **73**, 072003 (2006),
 156 doi:[10.1103/PhysRevD.73.072003](https://doi.org/10.1103/PhysRevD.73.072003).
- 157 [2] B. Abi *et al.* (Muon $g - 2$ collaboration), *Measurement of the Positive Muon*
 158 *Anomalous Magnetic Moment to 0.46 ppm*, Phys. Rev. Lett. **126**, 141801 (2021),
 159 doi:[10.1103/PhysRevLett.126.141801](https://doi.org/10.1103/PhysRevLett.126.141801).
- 160 [3] D. P. Aguillard *et al.* (The Muon $g - 2$ collaboration), *Measurement of the Positive*
 161 *Muon Anomalous Magnetic Moment to 0.20 ppm*, Phys. Rev. Lett. **131**, 161802 (2023),
 162 doi:[10.1103/PhysRevLett.131.161802](https://doi.org/10.1103/PhysRevLett.131.161802).
- 163 [4] D. P. Aguillard *et al.* (The Muon $g - 2$ collaboration), *Detailed Report on the*
 164 *Measurement of the Positive Muon Anomalous Magnetic Moment to 0.20 ppm*,
 165 doi:[10.48550/arXiv.2402.15410](https://doi.org/10.48550/arXiv.2402.15410). Accepted for publication on Phys. Rev. D.
- 166 [5] T. Aoyama *et al.*, *The anomalous magnetic moment of the muon in the Standard Model*, Phys.
 167 Rep. **887**, 1 (2020), doi:[10.1016/j.physrep.2020.07.006](https://doi.org/10.1016/j.physrep.2020.07.006).
- 168 [6] Sz. Borsanyi *et al.* (BMWc collaboration), *Leading hadronic contribution to the muon mag-*
 169 *netic moment from lattice QCD*, Nature **593**, 51 (2021), doi:[10.1038/s41586-021-03418-1](https://doi.org/10.1038/s41586-021-03418-1).
- 170 [7] F. V. Ignatov *et al.* (CMD-3 collaboration), *Measurement of the $e^+e^- \rightarrow \pi^+\pi^-$ cross section*
 172 *from threshold to 1.2 GeV with the CMD-3 detector*, doi:[10.48550/arXiv.2302.08834](https://doi.org/10.48550/arXiv.2302.08834).
- 173 [8] J. Grange *et al.* (E989 collaboration), *Muon $g - 2$ Technical Design Report*,
 174 doi:[10.48550/arXiv.1501.06858](https://doi.org/10.48550/arXiv.1501.06858).